International Journal of Engineering and Technology Innovation, vol. 15, no. 3, 2025, pp. 300-313

Uplift Capacity and Displacement of Pre-Bored PC Piles in Undrained Soils

Yit-Jin Chen[1], Mary Abigail Jos[1,*], Anjerick Topacio[2], Kai Wang[1]

[1]Department of Civil Engineering, Chung Yuan Christian University, Taoyuan, Taiwan, ROC

[2]Department of Engineering, Lyceum of the Philippines University - Cavite, Cavite, Philippines

Received 07 December 2024; received in revised form 13 April 2025; accepted 14 April 2025

DOI: https://doi.org/10.46604/ijeti.2024.14597

Abstract

This study aims to present interpretation recommendations to aid in the design of pre-bored PC piles in undrained soils, along with preliminary results for model factors to characterize model uncertainty. Measured capacities are estimated from the load-displacement curves using six interpretation methods, each assessed by employing the L2 method as a normalizing criterion. Predicted capacities are calculated via the α and β methods using analysis parameters for drilled shafts and are compared with measured capacities. Results show mean normalized capacities ranging from 0.45 to 1.60, with 6.4 to >43.9 mm displacements. A comparison of load-displacement behaviors reveals that pre-bored PC piles require greater displacements to mobilize the capacity than drilled shafts, driven piles, and barrette piles. The analysis highlights an overprediction of side resistance. Model factors, defined as the ratio of measured to predicted capacities, can calibrate resistance factors for reliability-based design.

Keywords: pre-bored PC piles, uplift load tests, load-displacement curves, interpretation criteria, analysis methods

1. Introduction

Driven piles and drilled shafts are widely utilized across the globe for pile foundations. Pre-bored PC piles have recently gained popularity due to their advantages, including reduced vibration and noise during construction. Additionally, the installation method of pre-bored PC piles, which provides moderate load-bearing capacity, involves inserting precast concrete piles into a pre-bored hole. The construction process of a pre-bored PC pile, as illustrated in Fig. 1, begins with using an auger drill to create a borehole to the required depth. During drilling, cement grout is injected to stabilize the surrounding soil. Subsequently, the precast pile is precisely lowered into the borehole [1].

Given that the construction method of pre-bored PC piles significantly differs from that of drilled and driven piles, their behavior requires a thorough evaluation. These differences in construction methods lead to variations in interface friction between the soil and the pile, as well as differences in bearing capacity and displacement. Therefore, the load-displacement behavior of pre-bored PC piles warrants further exploration. While extensive previous studies have been conducted to understand the uplift load-displacement behavior and side resistance of piles [2-5], the uplift behavior of pre-bored PC piles has rarely been investigated, indicating a research gap.

Several interpretation methods have been established for estimating uplift capacity from pile load tests; however, their applicability can vary across different types of piles. Previous studies on drilled shafts and driven piles have employed these methods for estimating pile capacity and have demonstrated that they represent various locations on the load-displacement curve, as well as different displacement ranges [4, 6-7]. Therefore, a thorough investigation is necessary to evaluate their effects on pre-bored PC piles in undrained soils under uplift loading.

* Corresponding author. E-mail address: g11172012@cycu.edu.tw

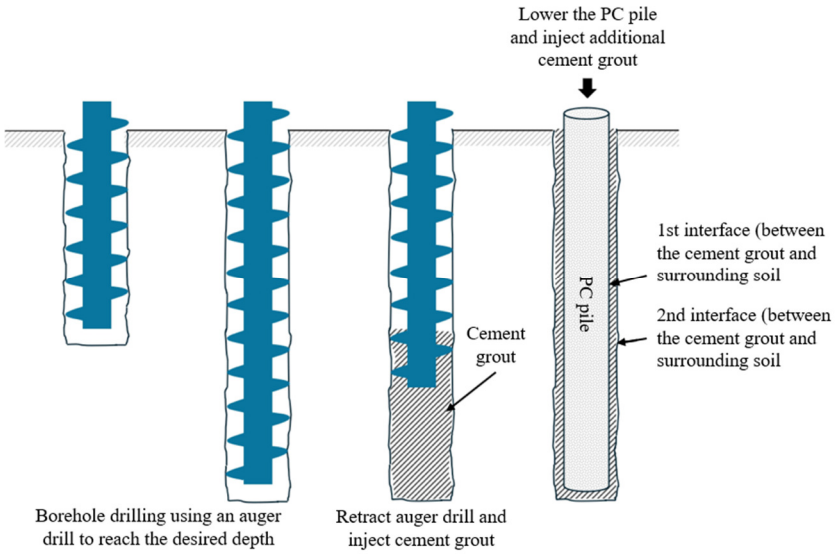

Fig. 1 Schematic diagram of pre-bored PC pile installation

In piles subjected to uplift loading, the total capacity is primarily influenced by side resistance, whereas the impact of the tip resistance is minimal [8]. As a result, side resistance analysis was employed to evaluate the theoretical capacity of piles under uplift conditions. The α and β methods are classical methods for analyzing the side resistance of a pile. The α method utilizes total stress analysis to evaluate side resistance in cohesive soils, relating side resistance to an empirical adhesion factor (α) associated with the average undrained shear strength (s_u) of the soil. The α value, originally proposed by Tomlinson [9], has been refined over time. For example, Chen et al. [3] updated the α value by correlating it with the s_u, obtained from consolidated-isotropically undrained triaxial compression (CIUC) tests. Conversely, the β method utilizes effective stress analysis to determine frictional resistance at the soil-pile interface. In this regard, several studies have applied this method to analyze the side resistance in undrained soils [3, 5, 8].

Migration from allowable stress design to reliability-based design (RBD) in geotechnical engineering began in the late 20th century [10]. At the core of the RBD is the objective of consistently achieving a designated reliability index (β) by maintaining factored loads below their corresponding factored capacities. The essential components of RBD include the characterization of geotechnical variability and model uncertainty. The simplest and most common approach for representing model uncertainty is to use the probabilistic distribution of the model factor. The introduction of model factors allows designers to calibrate RBD to consider geotechnical variabilities encountered during the design process.

A database of pre-bored PC pile uplift load tests in undrained soils available worldwide was utilized to evaluate their performance. Uplift capacities were estimated using interpretation methods, and the load–displacement behavior was analyzed and compared with that of other pile types under uplift loading. The measured capacities were compared with the predicted capacities calculated via traditional methods for calculating the side resistance. The ratio of measured capacities to predicted capacities, referred to as model factors, can be utilized in calibrating resistance factors for the RBD [10]. The probability distributions of model factors, including the mean and coefficient of variation (COV), are examined to provide insights into the comprehensive representation of model uncertainty. Based on the aforementioned analyses, this study presents interpretation recommendations to aid in designing pre-bored PC piles in undrained soils. Additionally, preliminary results for model factors are provided to characterize model uncertainty.

2. Measured and Predicted Capacities

This section discusses the methods employed in this study to determine the measured and predicted uplift capacities. Measured values were estimated through pile load tests using various interpretation criteria. Predicted capacities were calculated using established traditional methods for side resistance.

2.1. Interpretation criteria for measured capacities (Q_{sm})

Six representative uplift interpretation methods were utilized to determine the uplift capacity of pre-bored PC piles via available load test data. These methods can be categorized into three types: mathematical modeling, settlement limit, and graphical construction.

Within the mathematical modeling category, methods such as the Chin and van der Veen methods are included. These methods determine the uplift capacity by either extrapolating the load-displacement curve or applying logarithmic equations. In the Chin method, the load, Q_{CHIN}, is calculated as the inverse slope, $1 / m$, of the line $\rho / Q = m \times \rho + c$, where Q represents the load and ρ denotes total settlement [11]. In the van der Veen method, a plot is created by graphing total settlement against $\log (1 - Q / Q_{VDV})$ for different assumed values of ultimate load, where Q_{VDV} is the assumed ultimate load. The interpreted Q_{VDV} is determined as the value of the assumed ultimate load at which the plotted data best approximates a straight line [12]. The Fuller and Hoy method is included in the settlement limit group. The interpreted $Q_{F\&H}$ is defined as the minimum load corresponding to a total displacement rate of 0.05 inches per ton (equivalent to 0.14 mm/kN) [13].

The methods within the graphical construction group, including L_1–L_2, DeBeer, and slope–tangent, estimate capacity via load–displacement curves. As shown in Fig. 2, a typical load–displacement curve presents three distinct phases: initial linear, transition, and final linear regions. The key points on the curve highlight the elastic limit threshold, L_1, and failure threshold, L_2 [14]. Failure is qualitatively defined as the point when a small increase in load leads to a significant increase in displacement. The point L_1 corresponds to load, Q_{L1}, and displacement, ρ_{L1}. Meanwhile, the point L_2 corresponds to the load, Q_{L2}, and displacement, ρ_{L2}. The DeBeer method analyzes the log–log total displacement curve to identify the inflection point for changing slopes [15]. In the slope–tangent method, the load, Q_{ST}, is determined at a displacement that corresponds to the initial slope of the curve and an offset of 0.15 inches (equivalent to 3.8 mm), where B is the diameter [16]. These methods offer different approaches for determining the uplift capacity and interpreting the load–displacement behavior of pre-bored PC piles.

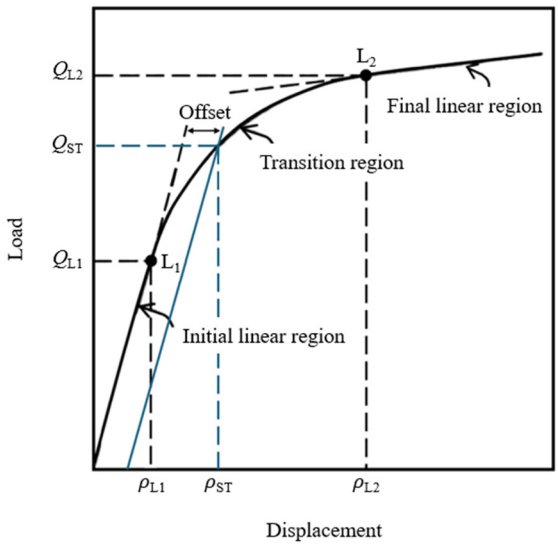

Fig. 2 Regions of load–displacement curve

2.2. Analysis methods for side resistance (Q_{sp})

The α and β methods have been extensively utilized to study the side resistance (Q_{sp}) of various pile types [3-5]. The formulas for calculating Q_{sp} using the α and β method, denoted as $Q_s(\alpha)$ and $Q_s(\beta)$ respectively, are given as follows.

$$Q_s(\alpha) = P\alpha s_u L \tag{1}$$

$$Q_s(\beta) = P\left(\frac{K}{K_o}\right)\sum_{n=1}^{N}\sigma'_{vo}K_o \tan\left(\phi' \times \frac{\delta}{\phi'}\right)t \tag{2}$$

where P is the perimeter of the pile, s_u denotes the undrained shear strength, α is the empirical adhesion factor, and L indicates pile length. Concerning calculations via the β method, K refers to the coefficient of horizontal soil stress, K_o represents the in-situ K, σ'_{vo} is the vertical effective stress, ϕ' is the effective stress friction angle, and δ is the soil-pile interface friction angle. The calculation is performed per layer, where t is the thickness of each layer. The $K/K_o = 0.79$ used in this study was adopted from the study of the Q_{sp} of drilled shafts [3], which is specific for slurry construction in undrained soils.

Similarly, the predicted α and β values are provided as follows, respectively.

$$Q_{\mathrm{CIUC}} = 0.32 + \left(0.16/s_u(\mathrm{CIUC})/p_a\right) \tag{3}$$

$$\beta_p = K_o\left(\frac{K}{K_o}\right)\tan\left(\phi' \times \frac{\delta}{\phi'}\right) \tag{4}$$

here, p_a denotes atmospheric pressure equal to 101.3 kN/m^2. The α_{CIUC} is adopted from a study on the uplift Q_{sp} of drilled shafts [3], which examined the correlation between α and s_u(CIUC), the s_u from a CIUC test.

3. Load Test Database

A database was established using pile load test results to assess Q_{sp} under undrained soil conditions. A total of six uplift load tests, primarily conducted in clay and currently available worldwide, were compiled for this study. Fig. 3 illustrates the load–displacement curves from each pile load test. Table 1 depicts the basic information and statistical results for each pile. The pile diameters ranged from 0.65 to 0.85 m, with pile lengths ranging from 40 to 62 m. The SPT-N values ranged from 3 to 11 blow counts, with a mean of 7 blow counts, indicating that the piles are embedded in clay with a consistency that varies from very soft to stiff [17]. The correlated shear strength for s_u(CIUC) ranged from 50.5 to 73 kN/m^2, with a mean value of 63.4 kN/m^2. The soil unit weight (γ) ranged from 18.11 to 18.50 kN/m^3, and the effective friction angle (ϕ') ranged from 14° to 27°, with mean values of 18.20 kN/m^3 and 21°, respectively. This useful database may be developed for applications in AI techniques in the future [18-19].

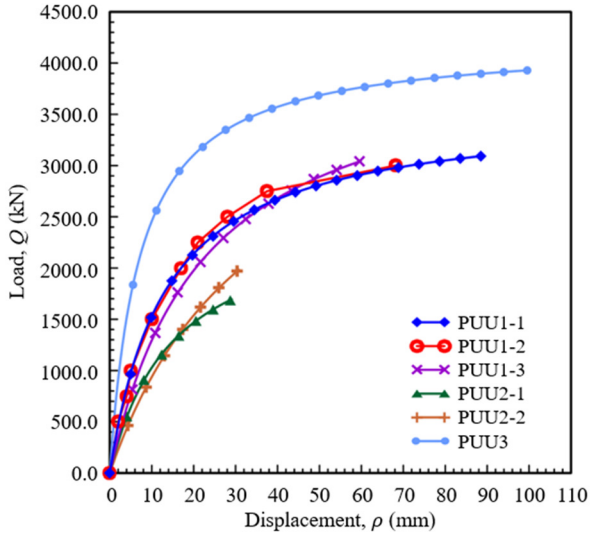

Fig. 3 Load-displacement curves of each pile

Table 1 Soil and pile information of undrained uplift load tests

Pile No.	PUU1-1	PUU1-2	PUU1-3	PUU2-1	PUU2-2	PUU3
Test location	Southeast China	Southeast China	Southeast China	Ningbo, China	Ningbo, China	China
Soil layer description	Silty clay	Silty clay	Silty clay	Soft clay	Soft clay	Silty clay
Pile diameter, B (m)	0.65	0.65	0.65	0.75	0.75	0.85

Table 1 Soil and pile information of undrained uplift load tests (continued)

Pile No.	PUU1-1	PUU1-2	PUU1-3	PUU2-1	PUU2-2	PUU3
Pile length, L (m)	43	43	43	40	40	62
L/B	66.15	66.15	66.15	53.33	53.33	72.94
GWT[a] (m)	0.5	0.5	0.5	0.0	0.0	1.0
SPT-N[b] (blow/ft)	11	11	11	4	4	3
γ[c] (kN/m^3)	18.11	18.11	18.11	18.19	18.19	18.50
s_u(CIUC)[d] (kN/m^2)	73.01	73.01	73.01	50.47	50.47	60.24
Ref[e]	[20]			[21]		[22]

Note: a – groundwater table, b – N value of standard penetration test, c – soil unit weight, d – undrained shear strength of soil for CIUC test, e – reference source of load test

Not all load tests provide specific geotechnical parameters, including s_u, which is essential for undrained Q_{sp} analysis. Therefore, some correlations between parameters must be determined. Given that most pile load tests report SPT-N values, a correlation was established between s_u and SPT-N, following the methodology of Terzaghi and Peck [23]. The s_u values were then converted to their equivalent CIUC values via the correlation proposed by Chen and Kulhawy [24].

4. Analysis Results of the Measured Capacities

This section presents the results of uplift capacities and the corresponding displacements, as determined using various interpretation criteria. The results are evaluated statistically and graphically to illustrate the applicability of each interpretation method to pre-bored PC piles in undrained soils.

4.1. Interpreted uplift capacities

The summary of loads or "capacities" obtained from different interpretation criteria, along with accompanying statistics including mean, standard deviation (SD), and COV, is presented in Table 2. The L_1 method yields the lowest interpreted capacities, with a mean capacity of 1,060 kN, an SD of 313 kN, and a COV of 0.29. The interpreted capacities of the other methods subsequently follow this order: the DeBeer method, with a mean interpreted capacity of 1,602 kN; the slope–tangent method, with a mean interpreted capacity of 1,747 kN; the van der Veen method, with a mean interpreted capacity of 2,232 kN; and the L_2 method, with a mean interpreted capacity of 2,380 kN. These methods are used to interpret capacities from the transition region to the beginning of the final region of the load–displacement curve. The Fuller and Hoy method and the Chin method interpret relatively large capacities, with Chin consistently providing the highest capacities owing to its calculation of the asymptote of the curve. The mean interpreted capacity using the Fuller and Hoy method is 2,626 kN, and the Chin method provides a mean interpreted capacity of 3,629 kN.

Table 2 Results of interpreted capacities

Pile No.	Diameter, B (m)	Length, L (m)	Interpreted capacity, Q (kN)						
			Q_{L1}*	Q_{DB}*	Q_{ST}*	Q_{VDV}*	Q_{L2}*	$Q_{F\&H}$*	Q_{CHIN}*
PUU1-1	0.65	43	1,300	1,654	1,870	2,380	2,500	>2,653[a]	3,578
PUU1-2	0.65	43	1,000	1,710	1,625	2,400	2,580	2,800	3,638
PUU1-3	0.65	43	1,000	1,500	1,980	2,460	2,550	2,810	4,200
PUU2-1	0.75	40	589	892	935	1,420	1,600	1,810	2,416
PUU2-2	0.75	40	890	1,210	1,320	1,700	1,650	>2,085[a]	4,004
PUU3	0.85	62	1,580	2,646	2,750	3,030	3,400	3,600	3,936
Mean	0.7	45.2	1,060	1,602	1,747	2,232	2,380	>2,626[a]	3,629
SD	0.1	7.6	313	543	567	529	614	573	582
COV	0.10	0.17	0.29	0.34	0.32	0.24	0.26	0.22	0.16

Note: a – data lies beyond extension curve, *: Q_{L1} – L_1 method, Q_{ST} – slope–tangent method, Q_{L2} – L_2 method, Q_{DB} – DeBeer method, Q_{VDV} – van der Veen method, $Q_{F\&H}$ – Fuller and Hoy method, Q_{CHIN} – Chin method

Each interpreted capacity and its corresponding displacement, as determined by the aforementioned methods, are illustrated in Fig. 4. Both Figs. 3 and 4 show notable scatter in the load–displacement points, which is expected due to variations in pile geometry and soil properties among different piles. Additionally, Fig. 4 (scatter values) and Table 2 (COV values) elucidate the variability inherent in the definitions and approaches of the various interpretation methods.

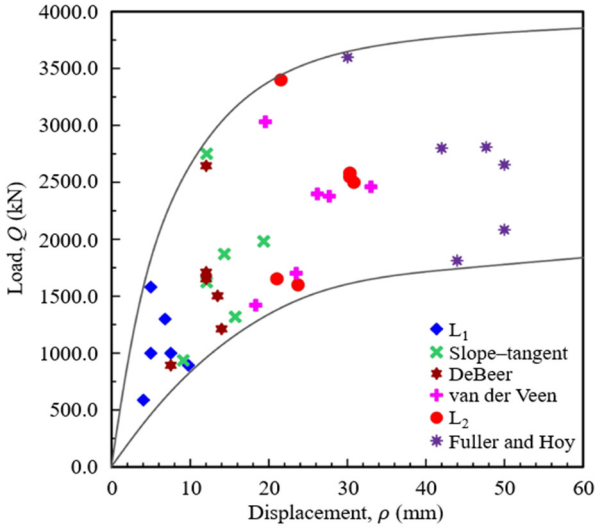

Fig. 4 Trend of load-displacement points using all interpretation methods

4.2. *Normalized interpreted uplift capacities*

Normalization is employed to evaluate the suitability of each method for pre-bored PC piles and to analyze their load–displacement behavior. This task entails normalizing each interpreted capacity against a reference value to enable standardized comparison among various interpretation methods. In this study, the L_2 method is chosen as the reference because of its favorable position on the load–displacement curve and its clear definition of the ultimate capacity [7, 14]. Previous studies assessing the behavior of various pile types have also utilized the L_2 method as a normalization criterion to enable comparisons of interpreted capacities derived from different methods [2-3, 7, 25], thereby demonstrating the effectiveness of this method.

Fig. 5 shows a scatterplot of the normalized capacities produced by each interpretation method. Notably, the scatter is significantly reduced compared with that in Fig. 4, highlighting the importance of standardization in the analysis and comparison of different interpretation methods. Normalizing the interpreted capacities via the L_2 method provides a more reliable basis for comparative analysis. Additionally, the COV for each normalized interpretation method is substantially lower than that of the unnormalized data, as detailed in Table 3.

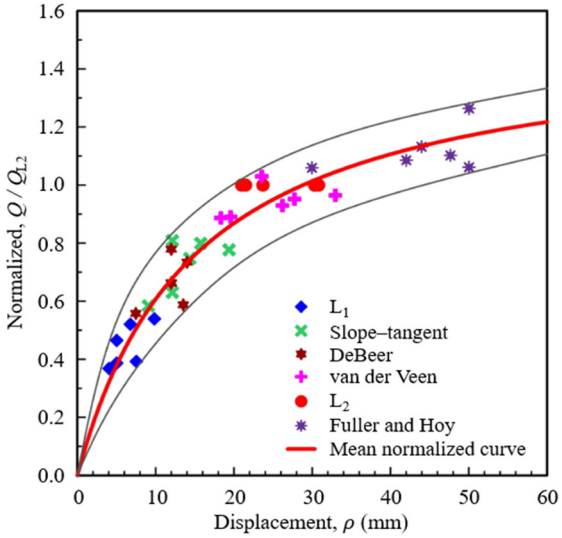

Fig. 5 Trend of normalized load-displacement points

Table 3 displays the results of the normalized capacities. The L_1 method produces the lowest mean normalized capacity of 0.45 and is situated in the initial linear region of the mean normalized curve. The elastic limit (L_1) is only half the failure threshold (L_2). Following this, the DeBeer and slope–tangent methods yield normalized capacities of 0.66 and 0.72, respectively. The results of the Fuller and Hoy method and the Chin method all exceed 1.00, which means they overestimate the capacity by 12% and 60%, respectively.

Table 3 Normalized load and interpreted displacements

Pile No.	Normalized load, Q/Q_{L2}						
	Q_{L1}*	Q_{DB}*	Q_{ST}*	Q_{VDV}*	Q_{L2}*	$Q_{F\&H}$*	Q_{CHIN}*
PUU1-1	0.52	0.66	0.75	0.95	1.00	>1.06[a]	1.43
PUU1-2	0.39	0.66	0.63	0.93	1.00	1.09	1.41
PUU1-3	0.39	0.59	0.78	0.96	1.00	1.10	1.65
PUU2-1	0.37	0.56	0.58	0.89	1.00	1.13	1.51
PUU2-2	0.54	0.73	0.80	1.03	1.00	>1.26[a]	2.43
PUU3	0.46	0.78	0.81	0.89	1.00	>1.06	1.16
Mean	0.45	0.66	0.72	0.94	1.00	>1.12[a]	1.60
SD	0.07	0.08	0.09	0.05	0.00	0.07	0.40
COV	0.15	0.11	0.12	0.05	0.00	0.06	0.25
Pile No.	Displacement, ρ (mm)						
	ρ_{L1}*	ρ_{DB}*	ρ_{ST}*	ρ_{VDV}*	ρ_{L2}*	$\rho_{F\&H}$*	ρ_{CHIN}*
PUU1-1	6.8	12.0	14.3	27.7	30.8	>50.0[a]	>50.0[a]
PUU1-2	5.0	12.0	12.1	26.2	30.3	42.0	>42.0[a]
PUU1-3	7.5	13.5	19.4	33.0	30.3	47.7	>47.7[a]
PUU2-1	4.0	7.5	9.1	18.3	23.7	44.0	>44.0[a]
PUU2-2	9.8	14.0	15.8	23.5	21.0	>50.0[a]	>50.0[a]
PUU3	5.0	12.0	12.1	19.6	21.5	30.0	>30.0[a]
Mean	6.4	11.8	13.8	24.7	26.3	>43.9[a]	>43.9[a]
SD	1.9	2.1	3.2	5.0	4.3	6.90	6.90
COV	0.30	0.18	0.23	0.20	0.16	0.16	0.16

Note: a – data lies beyond extension curve, *: Q_{L1}, ρ_{L1} – L_1 method, Q_{ST}, ρ_{ST} – slope–tangent method, Q_{L2}, ρ_{L2} – L_2 method, Q_{DB}, ρ_{DB} – DeBeer method, Q_{VDV}, ρ_{VDV} – van der Veen method, $Q_{F\&H}$, $\rho_{F\&H}$ – Fuller and Hoy method, Q_{CHIN}, ρ_{CHIN} – Chin method

4.3. Interpreted displacements

When the displacement at which loads are mobilized is elucidated, and the displacements associated with each interpreted load on the load-displacement curve are analyzed, designers can gain a more comprehensive insight into the effective application of load and displacement in their designs. The relative displacements for each uplift load test are shown in Table 3. This study defined a displacement limit to establish the maximum allowable displacement for the analysis of engineering practice. Since several load tests were terminated prematurely before failure, the dataset was considered right-censored. The interpreted failure load might not be identifiable beyond a certain displacement threshold. Statistics for these censored data can be derived via the maximum likelihood estimation method.

However, it is essential to determine a probability density function from the displacement values in Table 3. Chen et al. [25] adopted a straightforward approach by aligning the mean and median displacements, assuming a roughly symmetrical distribution. The displacement limit affects the mean and SD but not the median, provided that it remains below the limit. This approach established a reasonable displacement limit of 50 mm for this study. The L_1 method mobilized loads at an early stage, with a displacement of 6.4 mm; this is followed by the DeBeer, slope–tangent, van der Veen, and L_2 methods, which occur at displacements ranging from 11.8 to 26.3 mm. These methods mobilize capacities at the transition region to the beginning of

the final linear region of the mean normalized curve. They are appropriate for interpreting capacities for pre-bored PC pile design at the ultimate limit state. Conversely, the Fuller and Hoy method and the Chin method estimate capacities at relatively high displacements, exceeding 43.9 mm. Therefore, caution should be exercised when applying these two methods to pre-bored PC piles in undrained soils.

The mean normalized capacities and corresponding displacements, determined via the abovementioned interpretation methods, are plotted in Fig. 6 to show their positions on the mean normalized load-displacement curve. As expected, L_1 is positioned at the end of the linear elastic region. The Fuller and Hoy method is at the upper bound of the curve, and the other methods are positioned at the transition region to the final linear region of the curve.

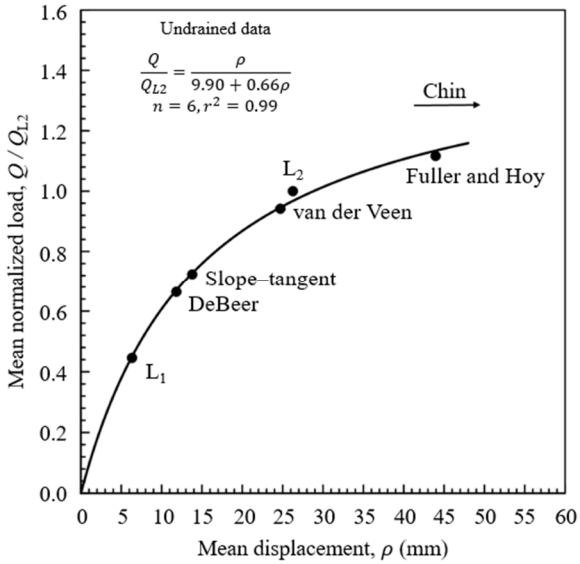

Q	Q / Q_{L2}	ρ (mm)
L_1	0.45	6.4
DeBeer	0.66	11.8
van der Veen	0.72	13.8
Slope–tangent	0.94	24.7
L_2	1.00	26.3
Fuller and Hoy	1.12	>43.9
Chin	1.60	>43.9

Fig. 6 Mean normalized load-displacement curve

4.4. *Various pile types under uplift loading*

Fig. 7 presents the mean normalized curves of different pile types under uplift loading. In addition to the data from this study, data for other pile types were sourced from other studies, namely, Chen et al. [2] for drilled shafts, Chen and Marcos [4] for driven piles, and Jos [26] for barrette piles. The pre-bored PC pile requires greater displacement before the capacity yields in the piles (Q/Q_{L2} = 1.0). One possible explanation for this behavior is that the cement grout acts as an intermediary material between the pile and the surrounding soil. This grout can influence the soil-pile interface dynamics.

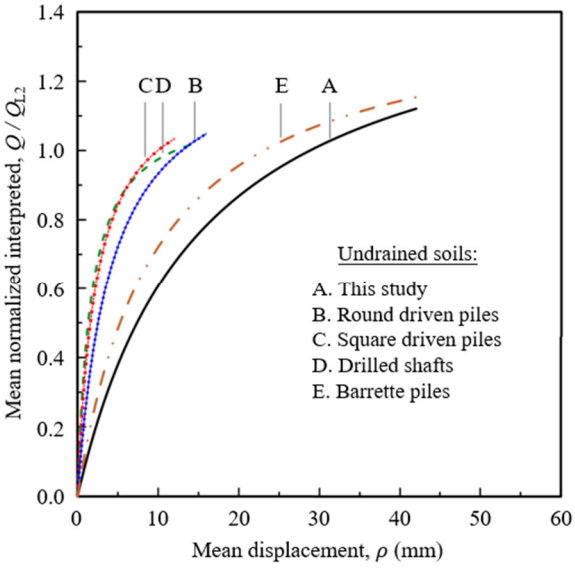

Study	B	L / B
A	0.65-0.85	53.3-72.9
B	0.40-0.60	15.0-86.0
C	0.30-0.40	21.0-124.2
D	0.35-1.52	1.6-56.0
E	1.60-2.47	17.0-29.1

Fig. 7 Mean normalized load–displacement curve for different pile types

Additionally, pre-bored PC piles are installed with less disturbance to the surrounding soil, which can result in reduced direct interaction between the soil and the pile. This reduced interaction often results in decreased frictional resistance or adhesion at the interface, in contrast to other pile types that are in direct contact with the soil. Consequently, with the reduced friction at the soil-pile interface, more displacement is required to effectively mobilize the uplift capacity of pre-bored PC piles than other pile types. However, Fig. 7 does not visually represent the relative strength of each compared dataset. Instead, it mainly illustrates the mobilized displacements of each L_2 capacity to analyze the differences in capacity mobilization between pre-bored PC piles and other pile types.

5. Analysis Results of the Predicted Side Resistance

The Q_{sp} was calculated using the α and β methods, and relevant geotechnical parameters were utilized for the analysis. The Q_{sp} were then compared with the Q_{sm} presented in the previous section, providing a basis for validation. Additionally, the findings were evaluated statistically and graphically and were compared with results from other piles under uplift loading.

5.1. α method

In the α method, the L_2 capacity was adopted as a reference for comparing the Q_{sp} and Q_{sm}. Table 4 presents the results of the Q_{sp} analysis via the α method. The predicted α values range from 0.54 to 0.64, whereas the back-calculated α values range from 0.34 to 0.40. The back-calculated α values are lower than the predicted values, primarily because the predicted α values are derived from the drilled shaft prediction model. Furthermore, the ratio of measured to predicted capacities has an average value of 0.64, which suggests an overprediction of the Q_{sp}.

Table 4 Predicted undrained side resistance using the α method

Pile No.	Pile length, L (m)	Perimeter (m)	L/B	s_u(CIUC)[a] (kN/m^2)	Q_{sm}[b] (kN)	Back-calculated	Predicted		Q_{sm}/Q_{sp}
						α_{CIUC}[c]	α_{CIUC}[d]	Q_{sp}[e] (kN)	
PUU1-1	43.00	2.04	66.2	73.01	2500	0.39	0.54	3475	0.72
PUU1-2	43.00	2.04	66.2	73.01	2580	0.40	0.54	3475	0.74
PUU1-3	43.00	2.04	66.2	73.01	2550	0.40	0.54	3475	0.73
PUU2-1	40.00	2.36	53.3	50.47	1600	0.34	0.64	3050	0.52
PUU2-2	40.00	2.36	53.3	50.47	1650	0.35	0.64	3050	0.54
PUU3	62.00	2.67	72.9	60.24	3400	0.34	0.59	5875	0.58
Mean	45.17	2.25	63.01	63.37	2380	0.37	0.58	3733	0.64
SD	7.65	0.23	7.25	10.18	614	0.03	0.04	977	0.09
COV	0.17	0.10	0.12	0.16	0.26	0.08	0.08	0.26	0.15

Note: a – undrained shear strength of soil for CIUC test, b – L_2 interpreted capacity or measured side resistance, c – back-calculated, d – 0.32 + [0.16 / (s_u(CIUC) / p_a)] from drilled shafts where p_a = atmospheric pressure 101.3 kN/m^2, e – predicted side resistance

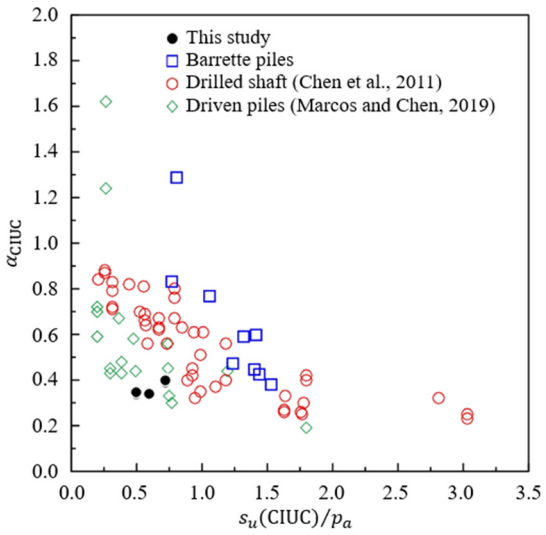

Fig. 8 α_{CIUC}-s_u(CIUC) / p_a points for different pile types

Fig. 8 presents the α_{CIUC}-s_u(CIUC) / p_a points for pre-bored PC piles in comparison to those of other pile types. These findings demonstrate that the α_{CIUC} values for pre-bored PC piles are generally lower than those of other pile types for equivalent s_u(CIUC) / p_a values. This lower range of α values may be ascribed to the presence of cement grout between the pile and the soil and the installation method for pre-bored PC piles. In contrast to drilled shafts and driven piles, pre-bored PC piles are installed with less disturbance to the surrounding soil, which can reduce direct soil–pile interactions and typically reduce adhesion. However, the data points somewhat overlap with those of the driven piles. Additional load test data are necessary to draw more definitive conclusions regarding the α_{CIUC}-s_u(CIUC) / p_a relationship for pre-bored PC piles under uplift loading. Further study may also be necessary to identify which of the two interfaces of the pre-bored PC pile plays a more significant role in governing side resistance.

5.2. *β method*

Table 5 presents the results of the Q_{sp} analysis via the β method. Estimated from the L_2 capacity, Q_{sm} varies from 1,600 to 3,400 kN, with a mean Q_{sm} of 2,380 kN, an SD of 614 kN, and a COV of 0.26. Conversely, Q_{sp} varies from 3,631 to 7,006 kN, yielding a mean predicted Q_{sp} of 4,265 kN, an SD of 1,228 kN, and a COV of 0.29. Notably, the Q_{sp} is generally overpredicted, with the predicted values exceeding the Q_{sm} by 57%.

Table 5 Predicted undrained side resistance using the β method

Pile No.	s_u(CIUC)[a] (kN/m^2)	ϕ'[b] (°)	OCR[c]	σ'_{vo}[d] (kN/m^2)	K_o[e]	β_m[f]	β_p[g]	β_m/β_p	Q_{sm}[h] (kN)	Q_{sp}[i] (kN)	Q_{sm}/Q_{sp}	Back-calculated (K/K_o)
PUU1-1	73.01	19	2.9	181	0.91	0.16	0.28	0.56	2,500	3,688	0.68	0.49
PUU1-2	73.01	19	3.0	181	0.93	0.17	0.29	0.57	2,580	3,819	0.68	0.50
PUU1-3	73.01	19	3.0	181	0.93	0.17	0.29	0.56	2,550	3,819	0.67	0.49
PUU2-1	50.47	27	1.5	160	0.64	0.11	0.26	0.40	1,600	3,631	0.44	0.32
PUU2-2	50.47	27	1.5	160	0.64	0.11	0.26	0.42	1,650	3,631	0.45	0.33
PUU3	60.24	14	1.2	272	0.77	0.08	0.15	0.51	3,400	7,006	0.49	0.38
Mean	63.37	21	2.17	189	0.81	0.13	0.25	0.50	2,380	4,265	0.57	0.42
SD	10.18	4.64	0.78	38	0.13	0.03	0.05	0.07	614	1,228	0.11	0.08
COV	0.16	0.22	0.36	0.20	0.16	0.26	0.19	0.14	0.26	0.29	0.19	0.18

Note: a – undrained shear strength of soil for CIUC test, b – soil effective friction angle, c – overconsolidation ratio, d – effective vertical overburden pressure, e – at-rest coefficient of horizontal soil stress, f – measured capacities, g – predicted capacities, h – measured side resistance, i – predicted side resistance calculated by β method

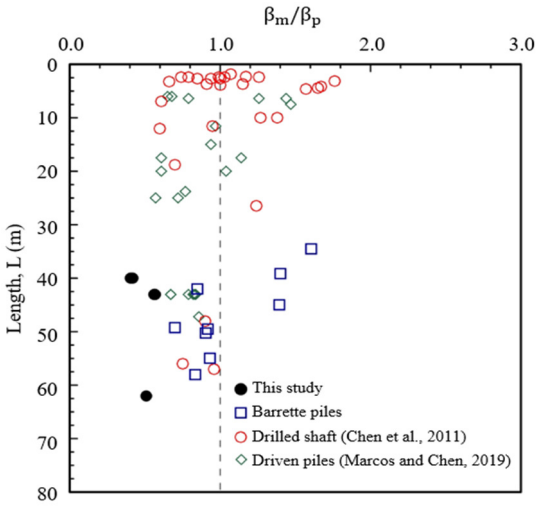

Fig. 9 β_m/β_p versus depth

Fig. 9 shows a comparison of the β_m/β_p ratios versus depth values for pre-bored PC piles alongside other pile types. The data indicate, within the same range of lengths, the β_m/β_p values of pre-bored PC piles fall between 0.40 and 0.57. The β_m/β_p values are notably lower than those observed for other pile types. One contributing factor to this overprediction is the adoption

of the K/K_o ratio derived from the Q_{sp} analysis of drilled shafts. The mean K/K_o value for this study is 0.42, although the load test data are limited. Additional uplift load test data could strengthen these findings. Both α and β methods overestimate the Q_{sp}. However, the α method is closely aligned with the Q_{sm} than the β method.

6. Normalization of the Interpretation Criteria by Measured Capacity

The measured-to-predicted capacity ratio is also known as the model factor. The probability distribution of the model factor is a widely used and straightforward approach for representing model uncertainty [10]. This approach involves determining the parameters of the probability distribution, specifically the mean model factor and COV. The mean model factor (bias) in terms of capacity can be categorized as either "conservative" or "unconservative." In particular, if the value is less than 1, then it is "unconservative"; if the value is between 1 and 3, it is "moderately conservative"; and if the value is greater than 3, then it is "highly conservative." [10].

Table 6 presents the results of the model factors from the α and β methods. For the α method, the mean model factors vary from 0.28 to 1.01, indicating unconservative values. The L_1 method has the lowest mean model factor, whereas the Chin method has the highest, being the only method where the Q_{sm} exceeds the predicted capacity. For the β method, the mean model factors range from 0.25 to 0.89, also indicating unconservative values. As shown in Fig. 10, the mean normalized curve of Q_{sm}/Q_{sp} versus displacement for both methods reveals that the L_1 method is still located in the initial linear region. In contrast, all other methods, except for the Chin method, fall in the transition to the final linear region of the curve.

Table 6 Ratio of measured versus predicted capacities (Q_{sm}/Q_{sp}) using α and β methods

Pile No.	Q_{sp}-α[a]	Q_{sm}/Q_{sp}						
		Q_{L1}*	Q_{L2}*	Q_{ST}*	Q_{DB}*	Q_{VDV}*	$Q_{F\&H}$*	Q_{CHIN}*
PUU1-1	3,475	0.37	0.72	0.54	0.48	0.68	0.76	1.03
PUU1-2	3,475	0.29	0.74	0.47	0.49	0.69	0.81	1.05
PUU1-3	3,475	0.29	0.73	0.57	0.43	0.71	0.81	1.21
PUU2-1	3,050	0.19	0.52	0.31	0.29	0.47	0.59	0.79
PUU2-2	3,050	0.29	0.54	0.43	0.40	0.56	0.68	1.31
PUU3	5,875	0.27	0.58	0.47	0.45	0.52	0.61	0.67
Mean	3,733	0.28	0.64	0.46	0.42	0.60	0.71	1.01
SD	977	0.05	0.09	0.08	0.07	0.09	0.09	0.22
COV	0.26	0.19	0.15	0.18	0.16	0.16	0.12	0.22
Pile No.	Q_{sp}-β[b]	Q_{sm}/Q_{sp}						
		Q_{L1}*	Q_{L2}*	Q_{ST}*	Q_{DB}*	Q_{VDV}*	$Q_{F\&H}$*	Q_{CHIN}*
PUU1-1	3,688	0.35	0.68	0.51	0.45	0.65	0.72	0.97
PUU1-2	3,819	0.26	0.68	0.43	0.45	0.63	0.73	0.95
PUU1-3	3,819	0.26	0.67	0.52	0.39	0.64	0.74	1.10
PUU2-1	3,631	0.16	0.44	0.26	0.25	0.39	0.50	0.67
PUU2-2	3,631	0.25	0.45	0.36	0.33	0.47	0.57	1.10
PUU3	7,006	0.23	0.49	0.39	0.38	0.43	0.51	0.56
Mean	4,265	0.25	0.57	0.41	0.37	0.53	0.63	0.89
SD	1,228	0.06	0.11	0.09	0.07	0.11	0.10	0.21
COV	0.29	0.22	0.19	0.22	0.19	0.20	0.16	0.23

*: Q_{L1} – L_1 method, Q_{ST} – slope-tangent method, Q_{DB} – DeBeer method, Q_{L2} – L_2 method, Q_{VDV} – van der Veen method, $Q_{F\&H}$ – Fuller and Hoy method, Q_{CHIN} – Chin method

The β method tends to possess lower model factors owing to its larger predicted capacities than those calculated via the α method. However, the results for the two methods are generally comparable and do not differ significantly. The range of the model factors is identical, and the trend and positioning of each interpretation method on the mean normalized curve are consistent. Model factors have also been determined to characterize model uncertainty in drilled shafts [9] and barrette piles

[27]. Tang and Phoon [10] compiled statistics of capacity model factors for various pile types, utilizing databases with ten or more load tests to minimize statistical uncertainty. This study yields preliminary results for the capacity model factors of pre-bored PC piles under uplift loading in undrained soils. The results can aid in calibrating resistance factors for the RBD. However, further load test data are recommended to increase the reliability of the findings.

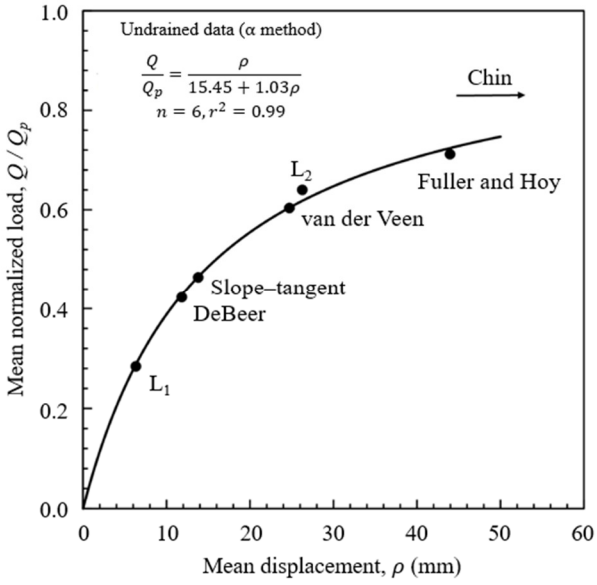

Q	Q / Q_p	ρ (mm)
L_1	0.28	6.4
DeBeer	0.42	11.8
van der Veen	0.46	13.8
Slope–tangent	0.60	24.7
L_2	0.64	26.3
Fuller and Hoy	0.71	43.9
Chin	1.01	>43.9

(a) α method

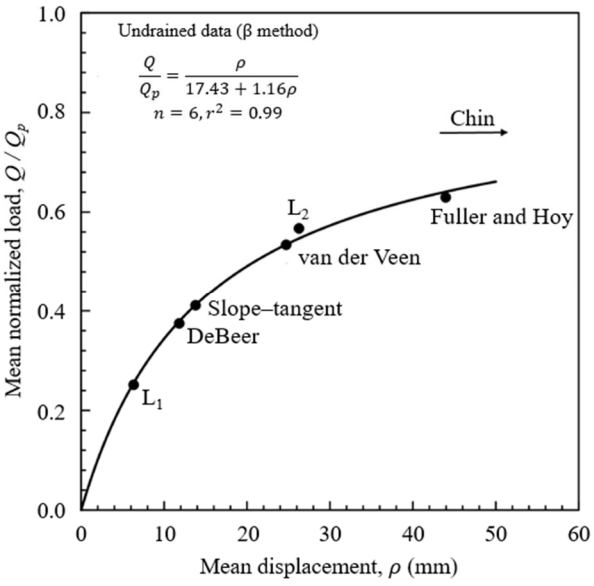

Q	Q / Q_p	ρ (mm)
L_1	0.25	6.4
DeBeer	0.37	11.8
Slope–tangent	0.41	13.8
van der Veen	0.53	24.7
L_2	0.57	26.3
Fuller and Hoy	0.63	43.9
Chin	0.89	>43.9

(b) β method

Fig. 10 Mean normalized load–displacement curves (Q_{sm}/Q_{sp})

7. Conclusions

This study analyzed uplift load test data from pre-bored PC piles in undrained soils. Q_{sm} were estimated from pile load tests using interpretation methods, whereas traditional models served as analysis methods to calculate the predicted Q_{sp}. Moreover, model factors for simplified RBD calibration were determined, leading to several conclusions and design recommendations.

(1) The L_1 method interprets uplift capacity at the initial linear region of the load-displacement curve at a mean displacement of 6.4 mm, making it suitable for serviceability design. In contrast, the Fuller and Hoy method and the Chin method overestimate the capacity by exceeding the curve's upper bound.

(2) The DeBeer, slope–tangent, van der Veen, and L_2 methods estimate capacities at the transition to the start of the final linear region of the curve, with mean displacements of 11.8 to 26.3 mm. These methods effectively estimate uplift capacity, with the specific choice depending on allowable displacements set by the design.

(3) Pre-bored PC piles require greater displacement to mobilize uplift capacity compared with other pile types, possibly due to the cement grout between the pile and the soil, and the installation method, which likely reduces direct soil–pile interactions.

(4) Back-calculated α_{CIUC} values range from 0.34 to 0.40, lower than those of other pile types, which may be attributed to reduced adhesion at the interface compared to piles in direct contact with the soil.

(5) A proposed stress factor of $K/K_o = 0.42$ for Q_{sp} analysis via the β method may address overprediction and be more applicable for pre-bored PC pile design. However, this value should be applied cautiously due to limited load test data.

(6) Both α and β methods overestimate Q_{sp}, with mean Q_{sm}/Q_{sp} values of 0.64 and 0.57, respectively. Future studies may focus on identifying which interface of the pre-bored PC pile significantly influences side resistance.

(7) The mean model factors are generally unconservative, with the Q_{sp} aligning closely with the Chin method. Preliminary capacity model factors for pre-bored PC piles are proposed for calibrating resistance factors in simplified RBD. Nevertheless, additional load test data are required to enhance the reliability of the findings.

Acknowledgments

The authors would like to express their gratitude for the support received from the National Science and Technology Council, Taiwan (NSTC 112-2221-E-033-022-MY3), and the John Su Foundation (CYCU 1120623).

Conflicts of Interest

The authors declare no conflict of interest.

References

[1] Q. Y. Yang, "Prebored P.C. Pile with Cement Milk," Sino-Geotechnics, no. 41, pp. 113-116, 1993. (In Chinese)
[2] Y. J. Chen, H. W. Chang, and F. H. Kulhawy, "Evaluation of Uplift Interpretation Criteria for Drilled Shaft Capacity," Journal of Geotechnical and Geoenvironmental Engineering, vol. 134, no. 10, pp. 1459-1468, 2008.
[3] Y. J. Chen, S. S. Lin, H. W. Chang, and M. C. Marcos, "Evaluation of Side Resistance Capacity for Drilled Shafts," Journal of Marine Science and Technology, vol. 19, no. 2, article no. 13, 2011.
[4] Y. J. Chen and M. C. M. Marcos, "Applicability of Various Load Test Interpretation Criteria in Measuring Driven Precast Concrete Pile Uplift Capacity," International Journal of Engineering and Technology Innovation, vol. 8, no. 2, pp. 118-132, 2018.
[5] K. K. Phoon, S. Laveti, Y. J. Chen, and M. A. Jos, "Evaluation of Side and Tip Resistances for Barrette Piles Using CYCU/Barrette/Side&Tip/64," Soils and Foundations, vol. 64, no. 3, article no. 101477, 2024.
[6] Y. J. Chen, K. K. Phoon, A. Topacio, and S. Laveti, "Uncertainty Analysis for Drilled Shaft Axial Behavior Using CYCU/DrilledShaft/143," Soils and Foundations, vol. 63, no. 4, article no. 101337, 2023.
[7] A. Topacio, Y. J. Chen, K. K. Phoon, and C. Tang, "Evaluation of Compression Interpretation Criteria for Drilled Shafts Socketed into Rocks," Proceedings of the Institution of Civil Engineers - Geotechnical Engineering, vol. 177, no. 1, pp. 17-33, 2024.
[8] M. C. Marcos and Y. J. Chen, "Evaluation of Side Resistance of Driven Precast Concrete Piles," IOP Conference Series: Materials Science and Engineering, vol. 658, no. 1, article no. 012005, 2019.
[9] M. J. Tomlinson, "The Adhesion of Piles Driven in Clay Soils," Proceedings of the 4th International Conference on Soil Mechanics and Foundation Engineering, pp. 66-71, 1957.
[10] C. Tang and K. K. Phoon, Model Uncertainties in Foundation Design, 1st ed., Boca Raton: CRC Press, 2021.

[11] F. K. Chin, "Estimation of the Ultimate Load of Piles from Tests Not Carried to Failure," Proceedings of Second Southeast Asian Conference on Soil Engineering, pp. 81-92, 1970.
[12] C. van der Veen, "The Bearing Capacity of a Pile," Proceedings of the 3rd International Conference on Soil Mechanics and Foundation Engineering, pp. 84-90, 1953.
[13] F. M. Fuller and H. E. Hoy, "Pile Load Tests Including Quick-Load Test Method, Conventional Methods, and Interpretations," Washington DC: Highway Research Record, vol. 333, pp. 74-86, 1970.
[14] A. Hirany and F. H. Kulhawy, "On the Interpretation of Drilled Foundation Load Test Results," Deep Foundations 2002: An International Perspective on Theory, Design, Construction, and Performance, pp. 1018-1028, 2002.
[15] E. E. de Beer, "Experimental Determination of the Shape Factors and the Bearing Capacity Factors of Sand," Géotechnique, vol. 20, no. 4, pp. 387-411, 1970.
[16] T. D. O'Rourke and F. H. Kulhawy, "Observations on Load Tests on Drilled Shafts," Drilled Piers and Caissons II, New York: ASCE, pp. 113-128, 1985.
[17] K. Szechy and L. Varga, Foundation Engineering: Soil Exploration and Spread Foundations, Budapest: Akademiai Kiado, 1978.
[18] C. J. Chen, T. W. Pai, J. L. Huang, Y. T. Lo, S. S. Lin, and C. C. Yeh, "Construction of a Metadata Schema for Medical Data in Networking Applications," 31st International Conference on Advanced Information Networking and Applications Workshops, pp. 597-600, 2017.
[19] Y. Chen, C. J. Chen, and C. J. Chen, "Schemes of Data Visualization for Ground Vibration Prediction Induced by Trains," Inter-Noise and NOISE-CON Congress and Conference Proceedings, vol. 258, no. 7, pp. 369-376, 2018.
[20] J. J. Zhou, J. L. Yu, X. N. Gong, R. H. Zhang, and T. L. Yan, "Influence of Soil Reinforcement on the Uplift Bearing Capacity of a Pre-Stressed High-Strength Concrete Pile Embedded in Clayey Soil," Soils and Foundations, vol. 59, no. 6, pp. 2367-2375, 2019.
[21] J. J. Zhou, X. N. Gong, K. H. Wang, R. H. Zhang, and J. J. Yan, "Testing and Modeling the Behavior of Pre-Bored Grouting Planted Piles under Compression and Tension," Acta Geotechnica, vol. 12, pp. 1061-1075, 2017.
[22] S. Huang, J. J. Zhou, X. N. Gong, J. L. Yu, J. Shu, and M. Wang, "Experimental Study on Bearing Capacity of Pre-bored Grouted Planted Pile under Compression and Tension," Journal of Hunan University Natural Sciences, vol. 48, no. 1, pp. 30-36, 2021. (In Chinese)
[23] K. Terzaghi and R. B. Peck, Soil Mechanics in Engineering Practice, 2nd ed., New York: John Wiley and Sons, 1967.
[24] Y. J. Chen and F. H. Kulhawy, "Undrained Strength Interrelationships among CIUC, UU, and UC Tests," Journal of Geotechnical Engineering, vol. 119, no. 11, pp. 1732-1750, 1993.
[25] Y. J. Chen, S. Laveti, M. A. Jos, and A. Topacio, "Database-Based Analysis of Compression Interpretation Criteria for Rectangular Barrette Pile Capacity," Soil Mechanics and Foundation Engineering, 2025, in press. https://doi.org/10.1007/s11204-025-10047-7
[26] M. A. Jos, "Evaluation of Side Resistance and Model Uncertainty Analysis for Barrette Piles and Pre-Bored PC Piles under Axial Uplift Loading," Master thesis, Department of Civil Engineering, Chung Yuan Christian University, Taoyuan, Taiwan, 2025.
[27] S. Laveti, Y. J. Chen, K. K. Phoon, and A. Topacio, "Evaluation of Model Factors for Barrette Piles Based on CYCU/Barrette/64," ASCE-ASME Journal of Risk and Uncertainty in Engineering Systems, Part A: Civil Engineering, vol. 10, no. 1, article no. 04023056, 2024.